Ambient Electron Density Derived from Differential Potential Measurements

Harri Laakso

Geophysical Research, Finnish Meteorological Institute, Helsinki, Finland

Arne Pedersen

Space Science Department, ESTEC/ESA, Noordwijk, The Netherlands

The potential difference, ΔV, between a satellite and an electric field probe is well correlated with the ambient electron density, n_e, in tenuous plasmas where the potential of the biased electric field probe can be kept close to that of the plasma nearly independently of n_e. Hence, ΔV is approximately equal to the satellite potential V_s. On the other hand, V_s is very sensitive to n_e as long as the satellite is positive with respect to the plasma potential. Therefore ΔV measurements provide a quite accurate diagnostic method for determining the bulk electron density in tenuous plasmas (i.e., below a few times 10 cm^{-3}). We present a numerical analysis of this technique under various plasma conditions. In particular we investigate how well n_e is determined from ΔV measurements when the ambient electron temperature, T_e, is not well known. It turns out that this relationship can be described by $\Delta V = 0.9\ T_{ph} \ln\left(0.15\ (a^2\sqrt{T_{ph}/I_b})n_e\right)$ (where I_b is the bias current, a is the probe radius, and T_{ph} is the photoelectron temperature).

INTRODUCTION

The electron density is one of the fundamental parameters in plasmas, and in tenuous plasmas its accurate and rapid determination is not always simple. A Langmuir probe, which can provide both the electron density and temperature, works well in plasmas where the electron density is a few electrons per cm^3 or more [*Hilgers et al.*, 1992]. Electron energy spectrum analyzers measure the electron velocity distribution function as a function of pitch angle and energy, and integration over pitch angle and velocity provides measurements of the bulk electron density [*Johnson et al.*, 1978]. However, the temporal resolution is limited (seconds at best), and often the cold population (< 10 eV) cannot be detected. The mutual impedance and plasma resonance sounder techniques provide accurate electron densities above a fraction of 1 cm^{-3}; time resolution is at best of the order of 1 second [*Decreau et al.*, 1978]. Finally, differential potential measurements with double probe experiments offer a simple, passive method of deriving bulk electron densities in the magnetosphere with a time resolution better than 0.1 s, as shown by numerous in-situ measurements with double probe antennas on satellites in the magnetosphere [see e.g., *Pedersen et al.*, 1984, 1991; *Pedersen*, 1995]. The capability and accuracy of this measurement technique is the subject of the present paper.

Double probe experiments, consisting of two identical conducting electrodes, yield a potential difference, $\Delta V_{12} = V_1 - V_2$, between the probes, which is related to a component of the average electric field along the instrument baseline. In addition to that potential difference, another potential difference, $V_2 - V_s$, between one probe (biased to V_2) and the spacecraft (floating at V_s for spacecraft with sufficiently conductive surfaces) is also sampled (Figure 1). In

Measurement Techniques in Space Plasmas: Particles
Geophysical Monograph 102

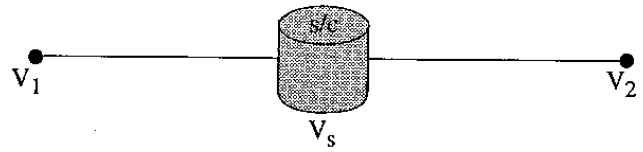

Figure 1. Configuration of a double probe experiment, composed of two spherical probes at the tips of two opposing booms. Both $V_1 - V_2$ and $V_2 - V_S$ are sampled.

tenuous plasmas, this difference is large and negative because V_S is large and positive, and V_2 is close to zero (due to the bias current driven to the probe). When the ambient electron density varies, V_S changes accordingly while V_2 remains relatively constant because of the bias current that is usually one or two orders of magnitude larger than the ambient electron current. Therefore this potential difference serves as a good estimate of the spacecraft potential, which is, on the other hand, related to the electron density. When V_2 is near zero or negative (that is, for plasma densities above a few hundreds electrons per cm^3, where the ambient electron current is comparable to or larger than the bias current), this technique fails.

This paper presents a numerical analysis of the capability and accuracy of the technique for determining the bulk electron density from potential difference measurements between spacecraft and one electric field probe. In particular we analyze how $\Delta V = V_S - V_2$ is related to the ambient electron density n_e and how this relationship is affected by such parameters as the ambient electron temperature, the photoelectron temperature, the saturation photoelectron current density, and the bias current. We also study the validity of this technique in plasma environments of other planets.

SURFACE VOLTAGE OF A BODY IN A PLASMA

When a conducting probe is immersed in a plasma, it acquires an equilibrium potential for which the sum of all the currents to the probe is zero; this potential is called the probe potential. In this paper we take into account the ambient electron current ($= I_e$), the ambient ion current ($= I_i$), the photoelectron current ($= I_{ph}$), and the bias current ($= I_b$). The probe potential is then obtained by solving $I_e + I_b - I_i - I_{ph} = 0$.

Electron and Ion Collection

Let us assume that the probes and the satellite are small compared with the Debye length, that the plasma is Maxwellian, that the ions are of one species, and that the electron temperature is equal to the ion temperature. For convenience, let us define the ambient plasma to be at zero potential. The current of ambient electrons collected by the probe, I_e, can be written [*Whipple*, 1981]

$$I_e = I_{e0} \exp\left(\frac{V}{V_e}\right), \quad V \le 0 \tag{1a}$$

$$I_e = I_{e0} G(V/V_e), \quad V \ge 0 \tag{1b}$$

where $I_{e0} = S\, e\, n_e \sqrt{eV_e/2\pi m_e}$, V is the probe potential relative to the ambient plasma, $V_e = T_e/e$, $S = 4\pi a^2$ is the surface area of the probe, a is the probe radius, e is the electron charge, n_e is the ambient electron density, m_e is the electron mass, and $G(V/V_e)$ is a function of the probe geometry. For a spherical probe, $G(x) = 1 + x$, where x is a free variable. In this paper $a = 4$ cm, commonly used as a probe radius.

Similarly, the ambient ion collection is described by the following equations: $I_i = I_{i0}[1 - V/V_e]$, for $V \le 0$, and $I_i = I_{i0} \exp(-V/V_e)$, for $V \ge 0$, where $I_{i0} = I_{e0}/M$, $M = \sqrt{m_i/m_e}$, and m_i is the ion mass (assuming that $n_e \approx n_i$). Since we investigate plasma regimes where the surface potential is positive with respect to the ambient plasma, the ion current is, however, insignificant for the value of the surface potential.

Photoelectron Current

Solar EUV radiation produces a fairly intense photoelectron flux from surfaces immersed in space plasmas at 1 AU. When the surface is negative with respect to the plasma, all the photoelectrons emitted can escape, resulting in a saturation photoelectron current, I_{ph0}, i.e.,

$$I_{ph} = I_{ph0} = \frac{S}{4} j_{ph0}, \quad V \le 0, \tag{2a}$$

where j_{ph0} is the saturation photoelectron current density. The last equality is exactly valid only for a spherical body.

When the probe lies at a positive potential with respect to the plasma, a flux of low-energy photoelectrons returns to the probe. This current depends on the probe potential and the energy distribution of photoelectrons. If the velocity distribution of photoelectrons is Maxwellian (T_{ph} is the photoelectron temperature, and $V_{ph} = T_{ph}/e$) and the size of the probe is smaller than the Debye length, I_{ph} can be written as follows [*Grard*, 1973]

$$I_{ph} = I_{ph0} \exp\left(-\frac{V}{V_{ph}}\right), \quad V \ge 0 \tag{2b}$$

The value of j_{ph0} is influenced by several factors, like solar activity, since the photoelectron current depends effec-

tively on the solar EUV photon flux. For instance, *Brace et al.* [1988] found that j_{ph0} at solar maximum is almost twice as large as j_{ph0} at solar minimum. In a dense atmosphere, with a high rate of heavy neutrals and ions, j_{ph0} reduces significantly, and it becomes close to or even drops below laboratory values [*Brace et al.*, 1988]. On the other hand, in deep space far above the atmosphere, all the surfaces seem to emit many more photoelectrons than previously expected; j_{ph0} can exceed even 8 nA cm^{-2} at 1 AU [*Pedersen*, 1995].

Bias Current

Accurate electric field measurements require that the probe-plasma impedance, $Z = dV/dI$, be as small as possible to ensure a good coupling to the plasma and insensitivity to spurious currents [*Pedersen et al.*, 1984; *Laakso et al.*, 1995]. The most favorable situation appears when the probe potential is a few volts positive with respect to the ambient plasma.

The use of a high impedance current source for a double probe antenna results in the forcing of a current from the probe to the spacecraft; this actually means that the current source produces an electron flux from the spacecraft to the probe. This current, called a bias current, I_b, strongly limits the large positive values of the probe potential which occur in tenuous plasmas and result in large Z (e.g., ~10^7 Ω, see *Laakso et al.* [1995]). For a spherical probe in a very tenuous plasma, the probe potential is approximately $V/V_{ph} = \ln(I_{ph0}/I_b)$. If $I_{ph0}/I_b = 2$, the potential is $V \approx 1.0$ volts if $V_{ph} = 1.5$ volts, whereas the potential of a nonbiased probe moves to much larger values. In this work, the bias current is given as a normalized bias current density j_b, where $I_{\geq} = (S/4)\, j_b$.

RELATIONSHIP OF ΔV AND n_e

Let us assume that the photoelectron characteristics of the satellite and the probes are $j_{ph0} = 4$ nA cm^{-2} and $T_{ph} = 1.5$ eV. The saturation photoelectron current I_{ph0} from a spherical probe of 4 cm radius is then ~200 nA. Let us further assume that the probes are biased by a 100 nA current (that is, $I_b = I_{ph0}/2$) from the probe to the satellite, which corresponds to $j_b = 2$ nA cm^{-2}. This is a negligible contribution to the satellite potential (e.g., I_{ph0} ~ 100,000 nA for a satellite of 1 m radius), and thus, I_b can be ignored in the current balance equation for the satellite potential.

Panel *a* of Figure 2 shows the magnitude of the satellite potential (that is, a body with no bias current) plotted against the ambient electron density n_e in the range of 10^{-1} to 10^3 cm^{-3} for electron temperatures T_e of 0.1, 1, 10, 100, and 1000 eV. The sign of the satellite potential V_s is positive at low densities and negative at high densities. V_s increases with decreasing n_e, and this correlation is fairly independent of T_e. Panel *b* shows a similar presentation for the magnitude of the probe potential V_2 (that is, a body with bias current). V_2 is almost constant below ~1 cm^{-3} and independent of T_e. Panel *c* displays the difference of these two potentials, $\Delta V = V_s - V_2$, which is always positive because V_2 is more negative than V_s unless the sign of the a bias current is changed. In general ΔV and V_s show a similar variation at low densities (i.e., below a few electrons per cm^3 for these photoelectron characteristics). Note that neither V_s nor V_2 is usually measured at the satellite. Figure 2 shows that in tenuous plasmas V_s, V_2, and ΔV are only weakly dependent on T_e, but as soon as V_2 is close to zero, ΔV begins to show strong T_e dependence. After that, ΔV cannot be used to estimate n_e. In the case of Figure 2, a useful correlation between ΔV and n_e exists up to densities of 5–100 cm^{-3}, depending on the value of T_e. With a higher value of j_{ph0}, this technique works even at somewhat higher densities.

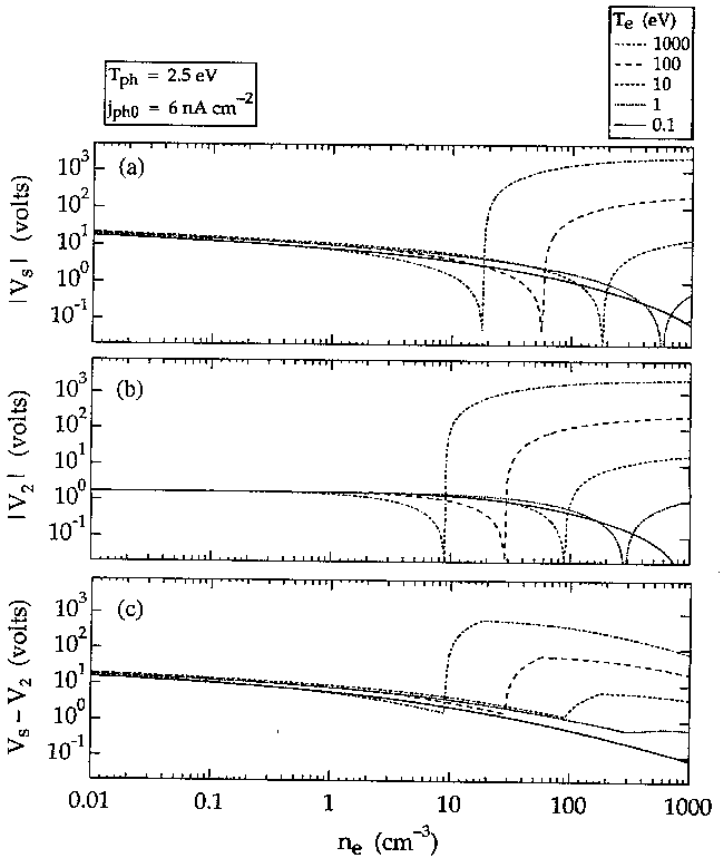

Figure 2. Magnitude of the satellite potential V_s (panel *a*) and the probe potential V_2 (panel *b*) plotted against the ambient electron density. Panel *c* shows the potential difference V_s–V_2. The ambient electron temperature is 0.1, 1, 10, 100 and 1000 eV. The photoemission characteristics are $j_{ph0} = 4$ nA cm^{-2} and $T_{ph} = 1.5$ eV. The bias current density is $j_b = 2$ nA cm^{-2}.

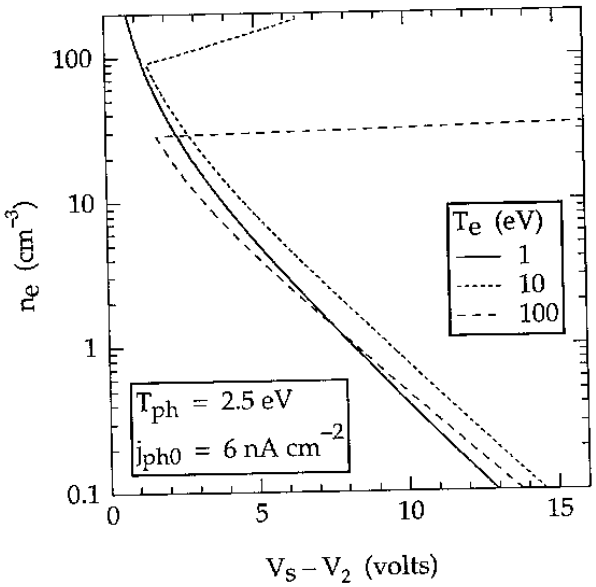

Figure 3. n_e *vs.* ΔV for electron temperatures of 1, 10, and 100 eV, when j_{ph0} is 4 nA cm^{-2} and T_{ph} is 1.5 eV. The linear relationship between n_e and ΔV is valid for n_e less than several tens of electrons per cm^3.

Figure 3 displays a part of the data shown in Figure 2*c*. Here n_e is plotted against ΔV for T_e equal to 1, 10, and 100 eV, which covers most of the plasma conditions encountered near the geosynchronous orbit. This figure indicates clearly that n_e can be determined fairly well from ΔV measurements without accurate knowledge of T_e (in the 1–100 eV range). Although this relationship fails when the biased probe becomes negative, this technique works up to densities of a few tens of electrons per cm^3.

According to Figure 3, log n_e and ΔV are linearly correlated in rarefied plasmas and therefore we attempt to find a more general expression for this correlation. The electron density is assumed to be between 10^{-1} and 10^3 cm^{-3}, and the electron temperature has 16 logarithmically-spaced T_e values in the 1–100 eV range. Figure 4 (*a*, *b*, *c*) plots n_e *vs.* ΔV. The photoelectron temperature T_{ph} is selected as (a) 1 V, (*b*) 2 eV, and (*c*) 3 eV. The other two instrument parameters are fixed: j_{ph0} = 6 nA cm^{-2} and j_b = 1 nA cm^{-2}. The linear correlation is obvious when n_e is below ~10 cm^{-3}. Furthermore, the n_e *vs.* ΔV relationship has a very clear dependence on T_{ph}, whereas no significant dependence on T_p exists.

Similarly, we have investigated how the log n_e vs. ΔV relationship depends on the other two parameters, j_{ph0} and j_b. Figure 5 presents three panels, for which j_{ph0} is (a) 4 nA cm^{-2}, (b) 6 nA cm^{-2}, and (c) 8 nA cm^{-2}. The other parameters are T_{ph} = 2 eV and j_b = 1 nA cm^{-2}. The values of the ambient plasma density and temperature are the same as in Figure 5. It may be somewhat surprising that the relationship between n_e and ΔV does not depend on the value of j_{ph0}. For instance, panels (a) and (c) are quite similar below 10 cm^{-3}, even though j_{ph0} is different by a factor 2.

Next we investigate the influence of I_b on the n_e *vs.* ΔV relationship. Figure 6 presents three cases where j_b is (a) 1 nA cm^{-2}, (b) 2 nA cm^{-2}, (c) 4 nA cm^{-2}, corresponding to 50 nA, 100 nA, and 200 nA bias currents, respectively. The photoelectron characteristics are j_{ph0} = 6 nA cm^{-2} and T_{ph} = 2 eV. Obviously the value of the bias current affect this relationship significantly.

In addition to Figures 4–6, we have examined a large number of cases where j_{ph0} ranges from 1 to 10 nA cm^{-2}, T_{ph} ranges from 1 to 5 eV, and j_b ranges from 1 to 4 nA cm^{-2}. In each case, we have determined the best fit to the data points. Investigation of these fits provides the following expression (as long as T_e lies in the range 1–100 eV):

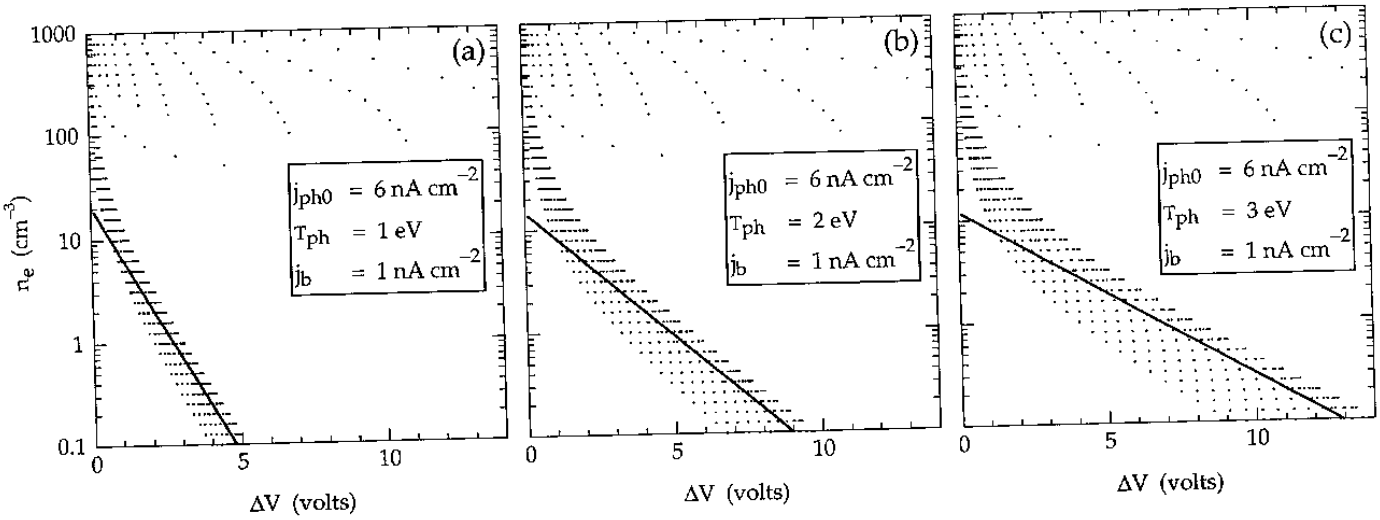

Figure 4. n_e *vs.* ΔV relationship for 16 T_e values in the range 1–100 eV, when T_{ph} is (*a*) 1 eV, (*b*) 2 eV, and (*c*) 3 eV. The other instrument parameters are j_{ph0} = 6 nA/cm^2 and j_b = 1 nA/cm^2. The solid lines represent Eq. (3).

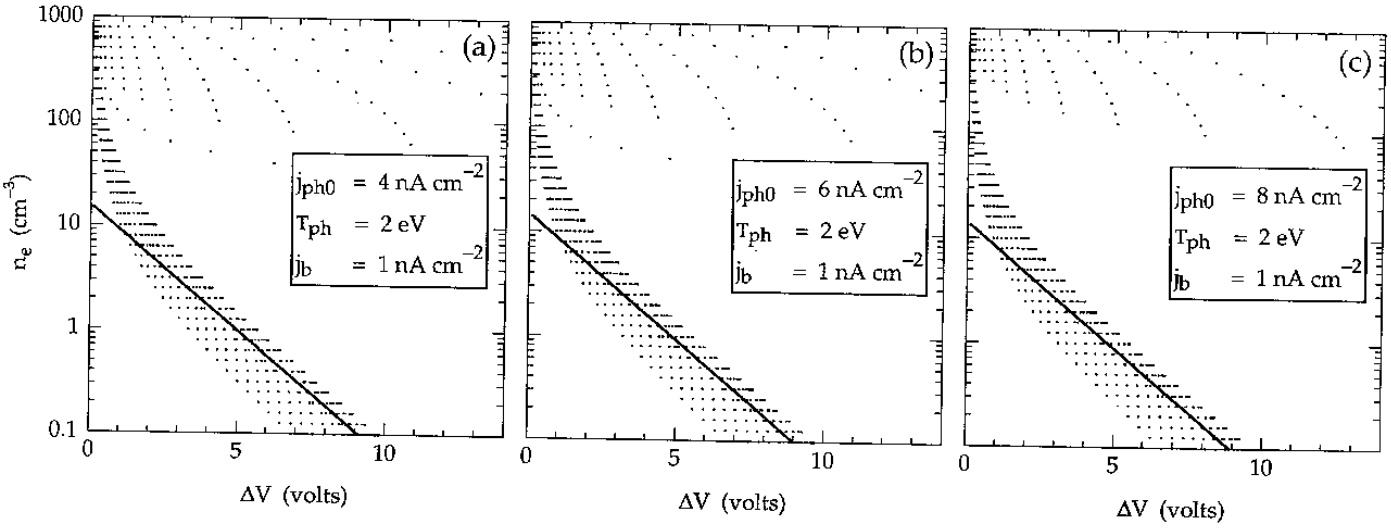

Figure 5. n_e *vs.* ΔV relationship for 16 T_e values in the range 1–100 eV, when j_{ph0} is (a) 4 nA/cm^2, (b) 6 nA/cm^2, and (c) 8 nA/cm^2. The other instrument parameters are T_{ph} = 2 eV and j_b = 1 nA/cm^2. The solid lines represent Eq. (3).

$$n_e \approx 6.6 \frac{I_b}{a^2\sqrt{T_{ph}}} \exp\left[-\frac{\Delta V}{0.9T_{ph}}\right] \text{ cm}^{-3}, \quad (3)$$

where I_b is given in nA, a in cm, and T_{ph} in eV. Equation (3) tells that at a given electron density, ΔV can be quite different depending on the value of the applied I_b current. The solid lines in Figures 4–6 represent this equation, showing that the agreement between the equation and the data points is reasonably good below ~10 cm^{-3}. We emphasize that the electron temperature T_e does not appear in (3). Ignoring T_e can cause an error that is at most of the order of ~25%, as long as T_e is in the 1–100 eV range.

DISCUSSION

The fact that the ambient electron density, n_e, and the potential difference, ΔV, between the satellite and a biased probe are closely correlated in tenuous plasmas has been exploited experimentally for long time (see e.g., *Pedersen* [1995], and references therein). Moreover, the value of the ambient electron temperature, T_e, does not significantly affect this relationship. This paper has presented a numerical analysis of this relationship and found that the n_e *vs.* ΔV relationship is affected by the value of T_{ph} and I_b, but is not affected by the value of j_{ph0}. Therefore, the utilization of the techniques described here does not require the knowledge of j_{ph0}, but rather the photoelectron temperature is more important. In fact, this paper assumes that the photoelectrons form a Maxwellian distribution, while in some cases, the velocity distribution function of photoelectrons is effectively bi-Maxwellian [*Laakso and Pedersen*, 1994; *Pedersen*, 1995]. How this finding affects the validity of expression (3) is a subject of a future study.

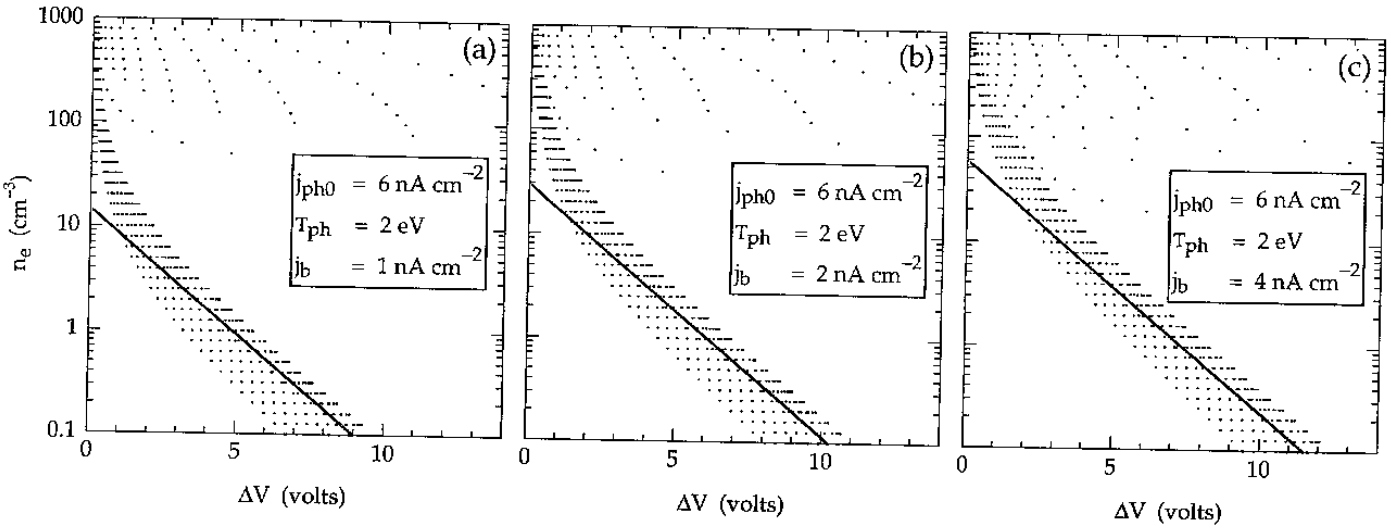

Figure 6. n_e *vs.* ΔV relationship for 16 T_e values in the range 1–100 eV, when j_b is (a) 1 nA/cm^2, (b) 2 nA/cm^2, and (c) 4 nA/cm^2. The other instrument parameters are j_{ph0} = 6 nA/cm^2 and T_{ph} = 2 eV. The solid lines represent Eq. (3).

The double probe technique has been and will be utilized in different plasma environments at different distances from the Sun. Therefore, we have investigated the n_e *vs.* ΔV relationship at other planets from Mercury to Saturn; the mean heliocentric distance, R, of the planets are: 0.387 AU (Mercury), 0.723 AU (Venus), 1 AU (Earth), 1.523 (Mars), 5.202 (Jupiter), and 9.538 AU (Saturn). Let us assume that the photoelectron characteristics at 1 AU are $j_{ph0} = 6$ nA cm^{-2} and $T_{ph} = 2$ eV. Then j_{ph0} at other planets is obtained by multiplying j_{ph0} at Earth by R^{-2}. The bias current density is selected to be $j_b = j_{ph0}/2$. Figure 7 presents the n_e *vs.* ΔV relationship for these planets, assuming that T_e is in the range 1–100 eV. As shown by this figure, this technique can be applied at Mercury for electron densities up to ~200 cm^{-3}. On the other hand, at Jupiter and Saturn, this technique is successful only up to a few electrons per cm^3. This is due to very low solar radiation and consequently low photoemission at large heliocentric distances, which causes a surface to float at a negative potential as soon as the electron density exceeds a few electrons cm^{-3}.

Finally, the utilization of expression (3) should be avoided when attempting to interpret variations in ΔV as electron density variations, unless the plasma and instrument parameters are in the range assumed in this paper. For instance, in the Earth's magnetotail, the electron temperature is in the 0.1–10 keV range. Panel c of Figure 2 clearly shows that a similar correlation between n_e and ΔV exist even in this temperature range. Hence, an expression similar to equation (3) can be found, only the multiplier 6.6 changes.

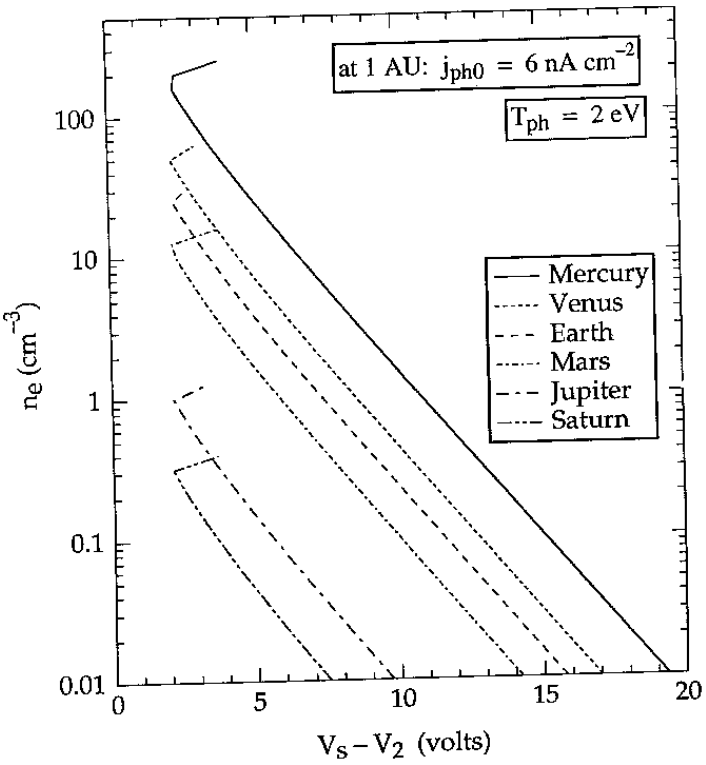

Figure 7. n_e *vs.* ΔV relationship for six planets from Mercury to Saturn. The photoelectron characteristics at 1 AU are $j_{ph0} = 6$ nA cm^{-2} and $T_{ph} = 2$ eV, and at other planets j_{ph0} is R^{-2}·6 nA cm^{-2}, where R is the planet's heliocentric distance. The bias current density $j_b = j_{ph0}/2$.

REFERENCES

Brace, L. H., W. R. Hoegy, and R. F. Theis, Solar EUV measurements at Venus based on photoelectron emission from the Pioneer Venus Langmuir probe, *J. Geophys. Res.*, *93*, 7282–7296, 1988.

Decreau, P. M. E., J. Etcheto, K. Knott, A. Pedersen, G. L. Wrenn, and D. T. Young, Multi-experiment determination of plasma density and temperature, *Space Sci. Rev.*, *22*, 633–645, 1978.

Grard, R. J. L., Properties of the satellite photoelectron sheath derived from photoemission laboratory measurements, *J. Geophys. Res.*, *78*, 2885–2906, 1973.

Hilgers, A., B. Holback, G. Holmgren, and R. Boström, Probe measurements of low plasma densities with applications to the auroral acceleration region and auroral kilometric radiation sources, *J. Geophys. Res.*, *97*, 8631–8641, 1992.

Johnson, J. F. E., J. J. Sojka, and G. L. Wrenn, Thermal/suprathermal plasmas observed by the S–302 experiment on GEOS–1, *Space Sci. Rev.*, *22*, 567–580, 1978.

Laakso, H. and A. Pedersen, Satellite photoemission characteristics, in *Materials in a Space Environment*, edited by H. T. D. Guyenne, pp. 361–365, ESA SP–368, ESTEC, Noordwijk, 1994.

Laakso, H., T. Aggson, and R. Pfaff, Plasma gradient effects on double probe measurements in the magnetosphere, *Ann. Geophys.*, *13*, 130–146, 1995.

Pedersen, A., Solar wind and magnetosphere plasma diagnostics by spacecraft electrostatic potential measurements, *Ann. Geophys.*, *13*, 118–129, 1995.

Pedersen, A., C. A. Cattell, C.-G. Fälthammar, V. Formisano, P.-A. Lindqvist, F. Mozer, and R. Torbert, Quasistatic electric field measurements with spherical double probes on the GEOS and ISEE satellites, *Space Sci. Rev.*, *37*, 269–312, 1984.

Pedersen, A., C. Nairn, R. Grard, and K. Schwingenschuh, Derivation of electron densities from differential potential measurements upstream and downstream of the bow shock and in the magnetosphere of Mars, *J. Geophys. Res.*, *96*, 11243–11252, 1991.

Whipple, E. C., Potentials of surfaces in space, *Rep. Prog. Phys.*, *44*, 1197-1250, 1981.

Harri Laakso, Geophysical Research, Finnish Meteorological Institute, P.O. Box 503, 00101 Helsinki, Finland

Arne Pedersen, Space Science Department, ESTEC/ESA, Postbus 299, NL–2200 AG Noordwijk, The Netherlands